AD-A072 587 NATIONAL OCEANIC AND ATMOSPHERIC ADMINISTRATION ANN --ETC F/G 8/10
NUMERICAL CASE STUDIES FOR OCEANIC THERMAL ANOMALIES WITH A DYN--ETC(U)
1979 J C HUANG

UNCLASSIFIED NL

1 OF 1
AD
A072587

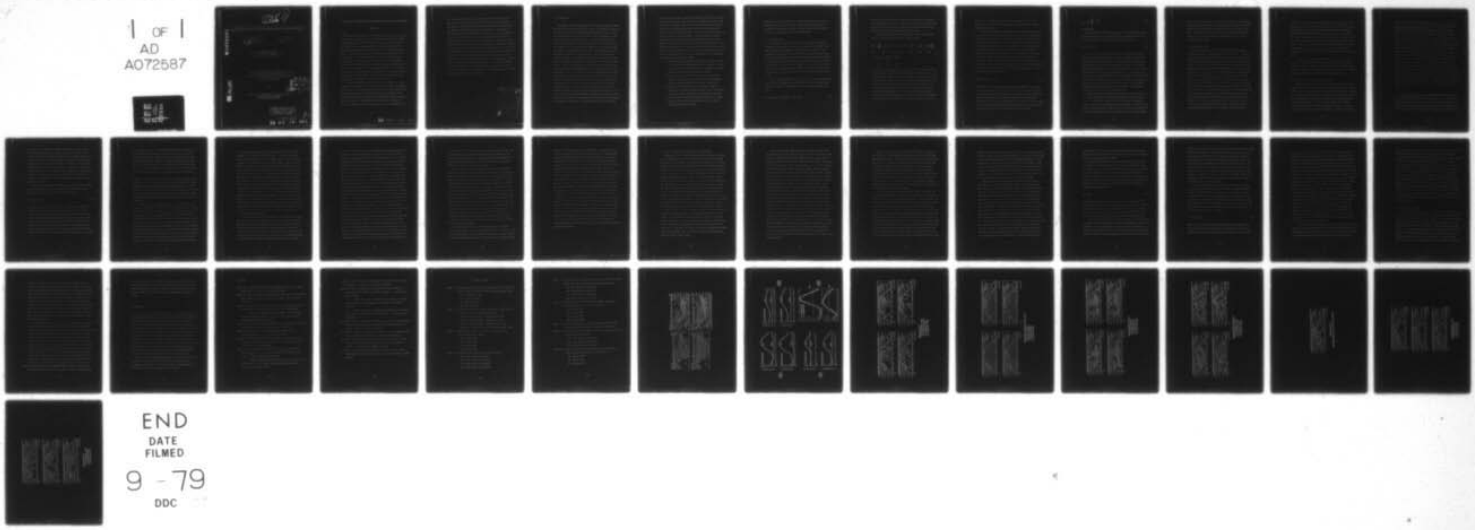

END
DATE
FILMED
9-79
DDC

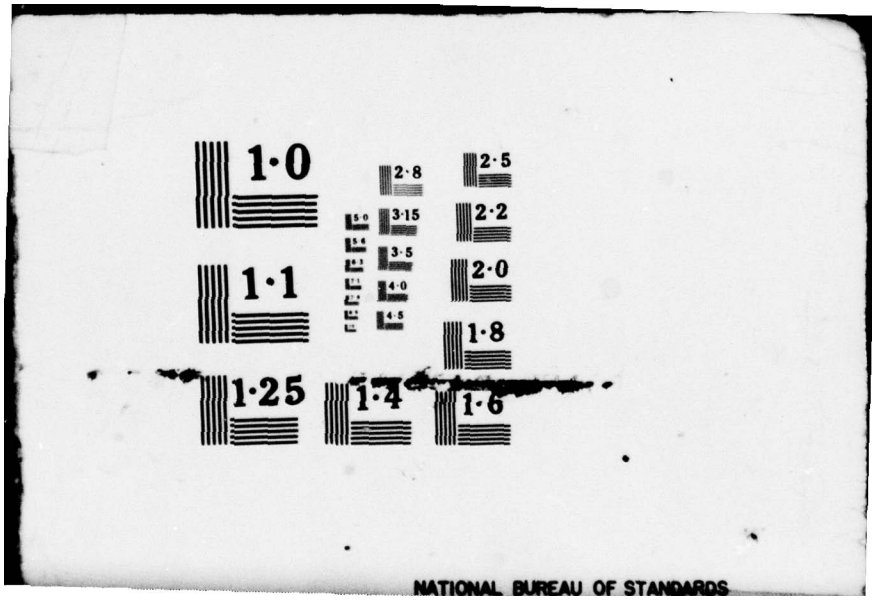
1·0
1·1
1·25
2·8
3·15
3·5
4·0
4·5
1·4
2·5
2·2
2·0
1·8
1·6
NATIONAL BUREAU OF STANDARDS

LEVEL II

NUMERICAL CASE STUDIES FOR OCEANIC THERMAL ANOMALIES WITH A DYNAMIC MODEL

(12) 41p. (11) 1979

(10) Joseph Chi Kan Huang

U.S. Department of Commerce
National Oceanic and Atmospheric Administration
Environmental Research Laboratories
Great Lakes Environmental Research Laboratory
2300 Washtenaw Avenue
Ann Arbor, Michigan 48104

and

Department of Atmospheric and Oceanic Sciences
The University of Michigan
Ann Arbor, Michigan 48109

NUMERICAL CASE STUDIES FOR OCEANIC THERMAL ANOMALIES WITH A DYNAMIC MODEL

Abstract

Numerical investigations to identify the physical processes responsible for the generation, evolution, and dissipation of oceanic thermal anomalies (OTA) were carried out using the numerical dynamic model of the North Pacific Experiment (NORPAX). The NORPAX model is based on time-integrations of the finite-difference forms of the primitive equations. It possesses an actual coastal configuration and 10 vertical layers, with a constant maximum depth of 4 km. The horizontal grid spacing, both longitudinal and latitudinal, is 2.5°. The seasonally varying model climatology is generated by integrating the model over 80 years of simulations under the climatological atmospheric forcing with the last 20 years varying with the seasonal cycle. Large-scale features of the model ocean climatology compare favorably with observed large-scale motions and structure in the North Pacific Ocean.

The model is used for oceanic thermal anomaly studies. Two simulated cases are presented: one demonstrates the generation and evolution of OTA's under anomalous atmospheric wind forcing of winter 1949-50, and the other portrays the evolution and dissipation of the OTA's under climatological atmospheric conditions in winter 1971-72. The resulting model simulations are compared with observational data to examine to what extent change of the oceanic thermal structure is accounted for by

the anomalous wind forcing and how much by the internal adjustments in the ocean. The model indicates that OTA's are generated by anomalous atmospheric winds and that thermal advection, both horizontal and vertical, plays the most important role in the generation. During winter, anomalous wind-induced upwelling has more influence on a cold anomaly in the tropic and subtropic regions than anomalous downwelling has on a warm anomaly in the subarctic region. The behavior of an initial anomaly under climatological conditions is closely related to large-scale features, such as the circulation pattern and the thermal gradient in the ocean, and is also subject to modifications due to the presence of OTS's. Most discrepancies found between the simulated and observed anomalies can be attributed to the lack of reliable and accurate meteorological and subsurface data. As better oceanic and atmospheric data become available, further studies of anomaly dynamics through numerical experiments will lead to understanding anomalous heat distributions in the upper layers of the ocean and hence to better ocean predictions.

1. Introduction

The purpose of this investigation is to identify the dominant physical processes in the ocean-atmospheric system responsible for the generation and evolution of oceanic thermal anomalies (OTA's) and to examine the thermodynamic balance in the interior of the ocean during and after the Oceanic thermal anomalies commence. A numerical dynamic oceanic model of the North Pacific Experiment (NORPAX) is used to carry out two case studies. The major objective of NORPAX is to understand the long-term (months to years) and large-scale (more than 100 km) fluctuations of physical variables in the North Pacific Ocean in relation to the overlying atmosphere. The emphasis has been on investigating the heat budget of the upper ocean and on the interaction of the atmosphere with the upper ocean. A numerical dynamic model of the North Pacific Basin has been developed by Huang (1978) as part of a program to achieve the NORPAX goals. The ocean model has the actual configuration of the North Pacific Basin in order to account for the large-scale waves due to the presence of realistic boundaries. Since the heat energy content in the upper layers of the ocean is very much affected by the lower layers, especially in the time scale of months to years, the ocean model also includes the processes of slow mixing and turning over of the deep ocean water. The model ocean has 10 variable thickness layers with a maximum constant depth of 4000 m. Horizontal grid separations, both longitudinal and latitudinal, are of 2.5°. The model ocean has been simulated for

more than 80 years under climatological forcing; the last 20 years have been the seasonal cycle. The simulated seasonally varying motions and structures in the North Pacific Ocean model are described and certain comparisons with observational data, especially in the mid-latitude region, are reported by Huang (1969). The present paper concentrates on two case studies of the low frequency transient behavior of oceanic anomalies in the North Pacific Ocean, with emphasis on the oceanic thermal structure, in response to prescribed atmospheric forcing. The OTA is the deviation of the temperature from the long-term mean value at the same location and time of year. This long-term mean value is referred to as the normal state, i.e., the climatology. We have addressed the following questions in this study:

a) Can OTA's be generated by normal atmospheric forcing when the ocean is already in equilibrium with the atmosphere? That is, will certain planetary wave phenomena excited by the seasonal forcing cause instabilities and generate OTA's?

b) Can OTA's be generated in the normal state ocean under an anomalous atmospheric forcing and what are the influencial dynamic mechanisms during and after their generations?

c) Will an existing OTA in the ocean propagate, evolve, and dissipate in a certain life span similar to those observed in the history of the ocean under normal atmospheric forcing?

d) Can the model simulate the observed evolution of an anomaly given the observed initial anomaly and the corresponding anomalous atmospheric forcing?

Only when the answer to (d) is yes, will model studies lead to better predictions for oceanic anomalies. However, owing to difficulties involved in preparing the required atmospheric data the present study focuses on answering only the first three questions.

2. Anomaly dynamics

A detailed description of the NORPAX ocean model, its boundary conditions, and forcing functions has been given in Huang (1978). The model is based on the complete nonlinear primitive equations. Both temperature and salinity are predicted from conservation equations and density is approximated as a linear function of temperature and salinity. While the grid size is small enough to resolve the large-scale OTA's, it is too large to resolve meso-scale eddies. There is no explicit mixed-layer dynamics incorporated in the model, except the vertical convective adjustment mechanism that is built in to ensure density stability in the ocean.

For seasonally varying phenomena in the ocean, a precise definition of anomaly is required. Let us define the anomaly of a time-dependent physical parameter, $q^*(x,y,z,t)$ as the deviation from its long-term mean

$$q^*(x,y,z,t) = q(x,y,z,t) - \bar{q}(x,y,z,t) \qquad (1)$$

where $\bar{q}$ (x,y,z,t) denotes the long term mean of q at the same geographical location and time of year. Therefore, an OTA for a given month and year is the devistion of that month's mean ocean temperature from the long term mean for that month averaged over many year.

The prediction equation for the OTA, after subtracting the long-term mean prediction equation of $\bar{T}$, can be written as

$$\frac{\partial T^*}{\partial t} = -\left[\bar{\mathbb{V}} \cdot \nabla T^* + \mathbb{V}^* \cdot \nabla \bar{T} + \mathbb{V}^* \cdot \nabla T^* + \bar{w}\ \frac{\partial T^*}{\partial z} + w^*\ \frac{\partial \bar{T}}{\partial z} + w^* \frac{\partial T^*}{\partial z}\right]$$

(a) (b) (c) (d) (e) (f) (g)

$$+ \kappa_1 \nabla^2 T^* + \kappa_2 \frac{\partial^2 T^*}{\partial z^2} + \delta\ (T^*), \tag{2}$$

(h) (e) (j)

where ∇ is the horizontal gradient operator; ∇^2, the horizontal Laplace operator; $\mathbb{V}$, the horizontal velocity and w, the vertical velocity. The physical interpretation of Eq. (2) is that the OTA will be generated by advection of the OTA by the normal current [term (b) and (e)]; by advection of the normal temperature distribution by the anomalous current [term (c) and (f)], and by the advection of the OTA by the anomalous current [term (d) and (g)]. It is also generated by non-advective processes [term (h) and (i)], such as horizontal and vertical diffusion of T*, anomalous surface heat fluxes due both to T* and to anomalous

atmospheric conditions. The last term [term (j)], is the convective adjustment of anomalous temperature due to instability in the vertical density stratification.

It is clear from Eq. (2) that if there exists no OTA at the initial state and no anomalous forcing at the air-sea interface, no OTA will be developed at a later time. In other words, no OTA's can be generated under normal atmospheric forcing from a normal model ocean where unexpected instability rarely occurs. However, OTA's can be generated either by anomalous heating [through term (i)] or by anomalous winds that produce anomalous current to advect the mean temperature field [through terms (c) and (f)]. In the upper ocean, the dominant wind-induced current is the Ekman-geostrophic current is the result of a horizontal gradient of density and/or surface elevation. Because of the hydrostatic approximation used in the model, the geostrophic current, Vg, satisfies the thermal wind relation, i.e.,

$$\frac{\partial Vg}{\partial z} = \frac{g}{f} \quad [k \times (\alpha \nabla T - \gamma \nabla S)] \tag{3}$$

where k is the unit vertical vector; g, the gravitational acceleration; f, the Coriolis parameter and α and γ, the thermal expansion coefficient and the haline contraction coefficient, respectively. Vg is obtained by vertical integration. The integration constant can be obtained by assuming that the vertical average of Vg is zero, which is consistent with the model definition of the baroclinic shear current. A geostrophic flow in the surface layers of the ocean induces a vertical motion

$$w_g = -\frac{\beta}{f}\int_z^0 v_g dz \qquad (4)$$

at the level z.

Near the bottom of the Ekman layer, the vertical velocity is mostly due to the divergence of the Ekman transport, depending directly on the vertical component of the curl of surface wind stresses, as

$$w_E = \hat{k} \cdot \nabla \times \frac{\vec{\tau}}{f} \quad . \qquad (5)$$

Horizontal and vertical advections can more effectively generate OTA's where the thermal gradients are strong. Therefore, ignoring the vertical mixing due to wind, OTA's can more often be generated in mid-latitude regions where the horizontal thermal gradients are strongest. The development of OTA by the horizontal displacement of oceanic fronts (Roden, 1976) is an extreme example of this process. In winter thermoclines are deep in high latitudes and relatively shallow in low latitudes. Wind-induced upwellings and downwellings are therefore more effective in the generation of OTA's in the tropics or subtropics than in middle or high latitudes mostely because of the f dependence in Ekman pumping, together with the relatively shallow thermocline.

Once the OTA is generated, all other therms in Eq. (2) come into play and the evolution of the OTA depends primarily upon the balance between the advective terms and the frictional terms, including the surface forcing. Namias (1965) made some approximate estimations of sea surface temperature (SST) anomalies from the anomalous horizontal advection of the mean normal temperature field and achieved a certain degree

of success as compared with the observed SST anomalies. Arthur (1966) and Jacob (1967) extended the OTA computation by including the advection of OTA by the normal and the anomalous currents [terms b and d in eq. (2)]. However, none of these early studies considered vertical advection (because of lack of sub-surface anomaly data) and none used a complete dynamical model.

3. Initial normal state

In the anomaly simulation experiments, the initial conditions consist of the model climatology plus a specified anomaly. The model climatology is the quasi-equilibrium state of the model after many years of time integration under a repeated annual cycle of seasonal forcing. The mean seasonal quasi-equilibrium state, after more than 80 years of integrations, has been presented by Huang (1969). The last model simulated year is considered to be the model climatology. As reported, the model has satisfactorily portrayed the gross features and seasonal variations in the North Pacific Ocean. The simulated results confirm that major seasonal fluctuations show mostly in the upper 350 m in the ocean. The model-produced seasonal SST generally matches the observed seasonal change as shown in figure 1, reproduced from Huang (1979), and the agreement is especially good in the mid-latitude North Pacific Ocean, the focus of the present study. Figure 2 shows both the simulated and observed seasonal variations of temperature at all three ocean weather stations, VICTOR (34°N, 164°E), PAPA (50°N, 145°N), and NOVEMBER (30°N, 140°W), where invaluable long time series of

temperature data are available in the North Pacific Ocean (Balis, 1973). Figure 2 also shows the seasonal variations of sea surface temperatures observed at two locations (45°N, 145°W and 21°N, 135°E) described by Wyntki (1968), together with the simulated sea surface temperature at the corresponding points in the model. In general, the simulated seasonal cycle of temperature fluctuation compare satisfactorily with observations. However, as pointed out (Huang, 1969), the simulated thermocline is deeper than the observed, which results in an understimate of the vertical advection of heat from the anomalous current [the f term in eq. (2)].

Since no OTA can be generated from the normal state ocean with normal atmsopheric forcing, we have concentrated on two cases in the anomaly experiments, namely the generation and evolution of OTA's under anomalous atmospheric forcing (case 1) and the evolution and dissipation of existing OTA's under normal atmospheric forcing (case 2).

4. Case 1: Generation and evolution of OTA's

Background. A typical case study for the generation and evolution of OTA's under the atmospheric anomalous forcing was selected for winter 1949-50. Namias (1951) and recently Dickson (1976) studied th atmospheric circulation related to the Great Pacific Anticyclone of winter 1949-50 to investigate its influence on storm tracks and anomalous weather over the United States. From early December 1949 to March 1950, a series of anticyclones formed in the eastern North Pacific, gyrated about a mean position and caused the mean mid-tropospheric circulation

pattern to evolute in an orderly fashion to become a vast warm anticyclone moving northwestward in a great arc from the southeast Pacific in December into the Bering Sea and to Canadina Yukon Territory by March. The continental United States suffered severe weather fluctuations, changing from anomalous cold in the west and anomalous warm in the east to a totally opposite pattern. Namias (1951) linked the abnormal weather in the United States to the anomalous flow pattern produced in part by the Great Pacific Anticyclone. Recently, Dickson (1976) reviewed the case and showed that this abnormal circulation pattern might have been influenced in its development and persistence by normal seasonal forcing as well as by the local SST anomaly gradient. The objective of this case study is to investigate whether OTS's can be generated by the observed anomalous wind forcing in the numerical model, how much is accounted for by the process of the surface stresses alone, and whether they evolve in a manner similar to the observed SST anomalies during this period of 1949-50, hence to identify the important physical processes and to determine how much is accounted for by the wind forcing alone. In this experiment there is no ocean anomaly at the initial time.

Anomalous atmospheric forcing. Monthly patterns of the sea level pressure anomaly for this case are shown in Figure 3. Data are kindly proviced by Namias' group at Scripps Institution of Oceanography. The data covers from 20° to 60° N and from 130° E to 110° W. A spline surface fitting on the data avoids possible abrupt changes outside of the

coverage area. As indicated in Figure 3a, the sea level pressure pattern in November 1949 shows an anomalous low in the northeast and an anomalous high in the central North Pacific. The anomaly shifted to an almost opposite pattern in December 1949 resulting in a Great Pacific Anticyclone in the eastern North Pacific. This high moved slowly northwestward, and intensified in January 1950. In general, a similar, but weaker, pattern persisted in February 1950, except that an anomalous low developed in the Gulf of Alaska region. Note that an anomalous low existed in the subtropic central North Pacific Ocean during the last 3 months of the period.

The anomalous geostrophic wind (Wg) over the middle-latitude region of the North Pacific Ocean is computed from the anomalous sea-level pressure distributions (P*) by the geostrophic relation,

$$Wg = \frac{1}{\rho_o f} \, k \times \nabla P^* \, . \qquad (6)$$

The local surface wind is obtained by rotating the geostrophic wind 15° to the left and reducing its magnitude by a factor of 0.8. Harmonic analysis is performed on the anomalous monthly mean wind computed from the pressure field of October, November and December 1949, and January, February and Marcy 1950, and null anomalies for the other months and three sets of Fourier coefficients are kept. The resulting anomalous wind, obtained from the harmonic coefficients, is added to the climatological wind to represent the total atmospheric wind forcing. As expected,

the combined winds show a strengthening in the westerly north of the anomalous high and a weakening south. Since there are no reliable anomalous heating data available for the time period of our interest, the anomalous heating is negledted as Namias (1951) did in his study. However, as the OTA develops, certain small amounts of anomalous heat flux is expected to develop in the model because it is the air temperature and not the heat flux that is prescribed. [See eq. (7) below.]

Results. There were no anomalies in the ocean at the beginning of the experiment. The experiment started on November 1 using the previously generated climatological model data and the integrations were carried out for 120 days under the combined anomalous wind forcing. The temperature and currents simulated in this experiment were converted to anomalies by simply subtracting the model seasonal climatology at the corresponding time.

The representative simulated anomalous oceanic surface layer currents for this period are shown in Figure 4, which indicates that Ekman dynamics dominate in the surface current. At the beginning, the anomalous surface currents are generally flowing southeastward as Ekman drifts in the eastern North Pacific north of 20° N and flowing northwestward in the Central Pacific Ocean as shown in Figure 4a, which is the surface current after 5 days of simulation in response to the anomalous wind induced from Figure 3a. As a result ther is weak horizontal divergence under the anomalous low and a weak convergence under the anomalous high during November. After 60 and 90 days, the simulated anomalous surface currents show a strong convergent pattern around the center of

the developing anomalous high and a weak divergent pattern around the subtropic low, as shown in Figures 4b and 4c. The surface anomalous flow is mostly northward in the eastern North Pacific and mostly northeastward in the western North Pacific north of 20°N. There are southward flows in high latitudes and in the western North Pacific near the western boundary. As a result of the horizontal convergence of the surface currents, downwellings are shown under the anomalous anticyclone in the subarctic and upwellings are indicated in the anomalous cyclone in the subtropics. Consequently, anomalously warm temperatures develop in the central and northeastern North Pacific and anomalously cold temperatures develop in the western North Pacific north of 30° N after 30 days simulation, as shown in Figure 5a. In the subtropics, warm OTA's are present in the east and west, but cold OTA's are present in the central North Pacific. The maximum warm anomaly is about 1° C and the minimum cold anomaly is about 0.7° C in the subtropics. Anomalies generated by anomalous surface winds do not penetrate at depth after 30 days. There is only an about 0.5° warm OTA shown at a depth of 60 m beneath the surface warm anomaly near 35° N.

Because of the intensifying atmospheric sea-level pressure anomaly the simulated OTA's become slightly more intense and deeper after 60 to 90 days (Fig. 5b and 5c), but generally have patterns similar to that of the first month. After 60 days of anomalous forcing, a warm OTA of about 0.6° appears in the eastern North Pacific Ocean at a depth of 100 m below the surface, and a sililar warm OTA of the same magnitude appears at 150 m depth after 90 days. No significant signal, i.e., and OTA

greater than 0.5° C, has ever appeared below 200 m depth throughout this experiment. For the last 30 days of integration, from day 90 to day 120, the anomalous wind shifts to a different pattern. As the anomalous anticyclone drifts westward and is replaced by an anomalous low in the Gulf of Alaska, more oceanic surface currents are directed toward the Bering Sea and a divergent flow is induced in the Gulf of Alaska (Figure 4d). Hence the cold OTA's in the western North Pacific near the Asian Continent diminish, while the cold OTA's along the eastern boundary are all extended and enhanced, as shown in Figure 5d. The persistent cold OTA in the subtropic region is the result of the anomalous low pressure in the region throughout the last 90 days. The observed SST anomalies for this period are shown in Figure 6. These SST anomalies are analysed by Namias' group based on data obtained from the National Marine Fishery Service. Though detailed comparisons between Figure 5 and 6 indicate no definitive resemblance, most large patterns show similar evolution and development with a pattern correlation coefficient of 0.63. Both the OTA at 10 m depth after 30 days' simulation and the observed SST anomalies of November 1949 show large pools of anomalously warm water in the middle and in the northeastern North Pacific Ocean, and anomalously cold water generally in the northwest and in the central subtropic North Pacific Ocean. However, the observed November warm OTA is split into two centers while the simulated anomaly is concentrated into one center. Though the simulated OTA's represent the anomalous temperature from the surface down to a depth of 20 m and their magnitudes are expected to be smaller than the surface temperature, the values of simulated OTA's, as

shown in Figure 5a, are about 30 percent lower than those observed. The overall weakness of all simulated anomalies may be attributed to the fact that the surface winds are computed from the smoothed monthly mean pressure anomalies, which results in weak surface stresses (Fofonoff, 1960) or to the absence of anomalous heating.

In the month of December, the general simulated anomaly pattern bears more resemblance to the observed one with a pattern correlation of 0.78. However the observed warm OTA centers have separated even more while the simulated anomaly simply expands somewhat in size. The same simulated pattern persists in January 1950 and resembles the observed pattern, except in magnitude, with a correlation coefficient of 0.72. These results indicate that in the high latitude region where the vertical thermal gradient is weak in winter, wind-induced downwellings under the imposed anticyclone do not show much efficiency in generating warm OTA's in the model. On the other hand, the wind-induced upwelling under the cyclone in the subtropic region generates cold anomalies most effectively as the depth of thermocline is relatively shallow and the Ekman pumping is relatively strong there. If the model is correct, the observed development of the warm anomaly in the Gulf of Alaska during December is most likely due to anomalous surface heat fluxes--an affect not considered in this study.

The observed SST anomalies are rather chaotic in the month of February 1950, and so is the simulated pattern with a correlation coefficient of 0.71, after the wind changed. They both have strong warm OTA's in the central North Pacific, and are generally warmer along the western

boundary, and colder along the eastern boundary. Considering the scarcity of observed data in the winter season three decades ago, detailed comparisons between the observation and the simulation are not very meaningful. To sum up, all we can say is that the simulation of the North Pacific Ocean under the observed anomalous atmospheric forcing has generated patterns of OTA's that qualitatively evolve in a manner similar to the observed SST anomalies with an overall pattern correlation coefficient of 0.72. This experiment has ascertained that the OTS's can be generated in a normal ocean under the anomalous wind forcing in the absence of heating and that they evolve realistically in the manner of the observed anomalies. In agreement with Namias (1965), results indicate that in the generation of OTA's, the anomalous advections of the normal temperature distributions, terms (c) and (f) in Eq. (2), play essential roles. They accounted for 38% (term c) and 17%, respectively, for the total 100% change of term (a) in the surface layer at the beginning of th experiment (the fifth day). Term (c) may be more important in mid-latitudes where the mean horizontal temperature gradient in the ocean is large while term (f) may be more important in low latitudes where the mean vertical gradient of temperature is large. In the subarctic where the horizontal and vertical temperature gradients are generally small, anomalous surface heat fluxes may be the most important generating mechanism.

5. Case 2: Evolution and dissipation of existing OTA's

Background. A case study to investigate the evolution and dissipation of existing OTA's is selected for fall and winter 1971-72 simply because it has been reported in numerous large-scale air-sea interaction studies (Namias, 1972; Dickson, 1972). Winter 1971-72 differed in many respects from the winters of the previous decade, not only in the severe weather patterns over the continental United States but also in the SST patterns over the North Pacific Ocean. The SST anomalies for winter 1971-72 were characterized by warmth in the eastern Central North Pacific and cold in the west coast of the United States, in contrast to those observed in earlier winters. However, once the new pattern was established, it persisted for a long period of time. Namias (1972) made objective predictions of the SST for this period by kinematic advection of the observed SST anomaly with the normal climatological winter currents [term (b) in (2)]. The results successfully indicated the eastward progression of the warm SST anomaly by the ambient surface current in the central Pacific. The present study attempts to hindcast the observed evolution and dissipation of the existing OTA's for winter 1971-72 by using a numerical model that contains the most essential dynamic and advective processes in the ocean and to compare hindcasts with observations to understand the thermodynamic balance in the interior of the model ocean. This particular winter case was also simulated numerically by Haney et al (1978) using a somewhat different model including the observed anomalous wind forcing.

The oceanic initial condition. The SST anomalies over the North Pacific Ocean for November 1971 are shown in Figure 7. This SST anomaly pattern is combined with the model climatology for 1 November of the normal seasonal state, to form the initial SST condition for this experiment. Because of the lack of subsurface data, it is necessary to specify the vertical profile of OTA's. According to White and Walker (1974), based on subsurface data from weather stations (PAPA, NOVEMBER, VICTOR), the OTA structure generally extends from the surface into the permanent pycnocline and the vertical profiles are generally homogeneous, though large variations and sometimes even reversed patterns exist. Their result also indicates that cold OTA's generally penetrate slightly deeper than warm anomalies. Based on these indications in the eastern and central North Pacific Ocean, where our major interest is focused, the penetrated depth of OTA's is assumed to be 225 m for the warm anomalies and 350 m for the cold anomalies, and they are set to be vertically homogeneous. Since the current in the model is found to adjust rapidly to the constraints of the specified density structure, no initial anomalous current pattern is imposed. Because emphasis is upon the evolution of observed OTA's, no anomalous atmospheric wind forcing is used in the experiment. The normal climatological conditions, reported in Huang (1969), are employed as forcing functions throughout the simulation. As will be discussed later, this imposed condition, which has ignored the anomalous wind forcing and introduced an anomalous heat flux, may have contributed to the discrepancy between the simulation and the observation.

Results. Integration was carried out for 120 days, starting from November 1 with the observed OTA's combined with the model climatology for appropriate layers. Due to the initial OTA, anomaly currents develop near the surface which generally flow anticyclonically around the warm anomaly in the middle of the North Pacific Ocean. This pattern of anomalous circulation persists, but gradually decreases in strength throughout the stimulation period. It is reasonable to expect that the cold anomalies in the western North pacific Ocean will be weakened as more warm water flows from the subtropics into the subartic reagion, while the cold anomalies along the eastern boundary will be strengthened as more subartic water flows southward.

Graphs on Figure 8 show the OTA's of the surface layer after 30 days, 60 days and 90 days of initial value integrations. Figures 8a, 8b and 9c show the corresponding 30, 60 and 90 day observed evolutions. As shown in Figure 8a, the OTA's in the surface layer have become everywhere weaker than the initial state after 30 days of simulation under the normal atmospheric forcing. The cold anomalous isotherms in the western North Pacific Ocean are pushed northward as indicated in Figure 8a. The anomalous isotherms in the eastern North Pacific close to the coast of the United States do not shown much change, except that they are slightly weaker than the initial state. The warm anomaly centered at 40° N, 170° W is shown to have drifted eastward about 6° of longitude and to have become similarly weaker. The warm anomaly center is further advected 3° -4° of longitude eastward after 60 days and,in addition to the general

weaking, the cold anomalies in mid-latitude close to the western boundary are pushed slowly northward along the Kuril Islands and the cold anomalies close to the eastern boundary are extended slightly southward, as shown in Figure 8b. A similar anomalous pattern persists for 90 days, except that the center of the warm anomaly has drifted southeastward and is now centered around 33° N, 160° W, as shown in Figure 8c. Notice that the temperature at the northwest corner, i.e., near the Bering Sea area, has also become slightly warmer than those of the previous months.

Figure 9a shows the corresponding SST anomaly pattern observed after 30 days. General agreement between Figures 8a and 8a is good, with a pattern correlation coefficient of 0.86. Both simulated and the observed anomalies have the same magnitudes and similar distributions. Slight discrepancies show at the centers of warm anomalies and in the southward extension of the cold anomalies near the eastern boundary. The central warm pool is observed to drift 11° eastward from November to December while the simulated movement is about 6° eastward. The observed cold anomalies also extend farther south in areas close to the Baja California coast. After 60 days, the observed SST anomaly pattern and the simulated OTA pattern still maintain major similarities except in the aforementioned two respects. The intensity of the southward extension of simulated cold anomalies in the eastern subtropics is also weaker than the observed, as indicated in Figure 8b. The same evolutionary tendency occurs in the third simulation month and similar patterns of discrepancies between the observed and the simulated anomalies exist

after 90 days. The center of the simulated warm anomaly is displaced about 11° of longitude eastward, while the observed center is displaced about 18° of longitude (Namias, 1972).

The major discrepancy between the simulated and observed anomaly intensities is probably due to different anomalous heat fluxes at the sea surface in the simulation and in the observed ocean. In the simulation, the surface heat flux is calculated in part from the climatological atmospheric air temperature. Because of this conditions, a sea surface temperature anomaly induces an anomalous heat flux which tends to damp the ocean anomaly. For typical atmospheric conditions, the induced anomalous heat flux if

$$H^* = QT^* \tag{7}$$

where T^* is the surface temperature anomaly and $Q = 70$ ly day^{-1} deg^{-1} (Haney, 1971). If the flux is taken out of a layer ΔZ meters thick, the resulting e-folding time is $\rho_o C_p \Delta Z/Q$ which is of the order of 100 days if $\Delta Z \simeq 70$m. Thus, the surface anomaly can be damped considerably by this mechanism during the 3 month integration period of this study.

It is also possible that the observed anomalous heat flux played an important role in maintaining and affecting the evolution of the observed anomalies. The air-sea interactions, initiated from the SST anomaly pattern of winter 1971-72, call for a likely anomalous atmospheric flow pattern consisted of anomalous northerly winds to the east of 160° W and

anomalous southerly winds to the west. The anomalous heat flux associated with the southerly wind is likely to have strengthened the warm anomaly in the eastern North Pacific Ocean and the northerly wind is likely to have enhanced the cold anomalies along with the California coast. The study by Haney it al (1978) suggests that horizontal advection by anomalous wind drived surface (Ekman) currents may have contributed to the anomaly development. It should be noted that the present model, having salinity as a dependent variable, is able to successfully simulate cold anomalies at high latitudes during winter whereas the model of Haney et al (1978), having no salinity, cannot.

The discrepancy in the eastward displacement of the warm anomaly center may be attributed to different mechanisms. Haney et al (1978) has shown using an idealized rectangular ocean model that a shallow anomaly will tend to be nearly stationary and a deep anomaly will tend to propagate westward under climatological atmospheric forcing. Based on the hydrostatic geostrophic relation, the large-scale thermal anomaly is generally propagating at an equivalent speed of C in the absence of anomalous forcing (Haney et al. 1978).

$$C = \bar{U} + C'_H + C'_V \tag{8}$$

where $\bar{U}$ is the mean zonal current speed, C'_H is the equivalent of the effect of the horizontal advection of mean temperature caused by the anomalous geostrophic current, and C'_V is the equivalent of the effect

of the vertical advection of mean temperature caused by the horizontal convergence of the anomalous geostrophic current. Both C'_H and C'_V are directly proportional to the depth of the thermal anomaly and both are negative in the mid-latitude of the North Pacific Ocean. It is the net effect of these three major advective components due to the zonal mean and anomalous currents, which determines the actual movement of the warm anomaly. The simulated movement of the warm anomaly containing a vertical depth of 225 m in our experiment still demonstrates an eastward propagation of about 14 cm s^{-1}. The average surface layer speed of the model wind-drift North Pacific current in the west and the central North Pacific is just slightly above this speed, about 2-3 cm s^{-1} higher. This shows that the effects of the anomalous advective propagations of the mean thermal field, namely, C'_H and C'_V are small when the warm anomaly is above 225 m in depth. The competing nature of these opposing mechanisms is clearly indicated since the eastward motion was even slower in the last 30 days of simulation (only 2° of longitude per month), as the center of the warm anomaly migrated further south to about 32° N, where the eastward North Pacific current is weaker than that along 40° N. The eastward movement in the deeper layers is also slower than that in the surface layer.

It is felt that the simulation has been successfully used to investigate the evolution and dissipation of an existing OTA under the normal atmospheric forcing in the North Pacific Ocean. The anomaly simulation has qualitatively portrayed the development of OTA's, both cold and

warm, and captured major part of the eastward moving characteristics of the mid-latitude anomalies. The discrepancy between simulation and observation appears to be due to either anomalous wind or thermal forcing (neither of which were correctly incorporated) or to an inadequate specification of the sub-surface structure of the anomalies. It was shown that sufficiently deep anomalies can persist for a long period of time without much dissipation (at least 120 days) and still maintain more than half of their original strengths in a recognizable pattern under normal atmospheric forcing. Evolutions and developments of OTA's depend in part upon the large-scale kinematic and dynamic characteristics in the ocean which have been simulated in this study. As indicated in case 1, since the ocean and the atmosphere are mutually coupled and continually interacting, OTA's are subject to continuous modifications from the atmosphere, which may have just updated its status due to feedbacks from the ocean.

6. Conclusions and remarks

Numerical studies to investigate the generation, evolution and dissipation of OTA's in the North Pacific Ocean have been carried out with the NORPAX dynamic model. This paper reports on two numerical simulation experiments using observed atmospheric and SST anomalies; one for the generation evolution of OTA's under the anomalous wind forcing and the other for the evolution and dissipation of an existing OTA under climatological atmospheric conditions. In the first simulation there was no OTA at the initial time while in the second case an observed OTA is specified down to 225 m. Integrations were carried out for 120 days in

both cases. Results of case 1 show that OTA's are generated by the anomalous wind through wind-induced advections of normal thermal distribution. Vertical advection play important roles in OTA generations and their later developments, especially in the tropic and subtropic regions during the winter when the thermocline is relatively shallow and the Ekman pumping is relatively strong there. The simulated OTA's evolve similarly to the observed SST anomaly for winter 1949-50, with an overall pattern correlation coefficient of 0.72. The study of case 2 indicates that under the assumed boundary conditions, the existing OTA's decrease exponentially in time [see eq. (7)] with typical e-folding time scales of the order of 100 days.

The simulation of case 2 has qualitatively portrayed the evolution of existing OTA's which evolve and develop in a rather realistic and orderly fashion related closely to the general features of the circulation and the anomalous current induced by the OTA's. However, as expected, it does not produce exactly the observed SST anomaly pattern, missing the pronounced increase in the intensity of anomalies. The fact that the observed anomalies intensified during winter 1971-72 is attributable mostly to the anomalous atmospheric forcing which was not properly taken into account in this experiment. The simulation also does not capture exactly the eastward movement of the observed warm anomaly, but shows a slower speed. This discrepancy may be due to the neglect of anomalous wind forcing in the model or to the inadequate specification of the subsurface structure of the initial OTA's. In high latitude regions, the salinity anomaly may also be important. Accurate three-dimensional

surface and subsurface data on OTA's and salinity anomalies as well as anomalous meteorological forcing data, both wind stress and heating, are greatly needed for more realistic anomaly simulations in the ocean. An important start in that direction has been made by White and Bernstein (1978).

Acknowledgments

The author wishes to thank J. Namias, W. B. White and R. M. Born of the Scripps Institution of Oceanography; R. R. Dickson of the Fishery's Laboratory of the British Directorate of Fisheries Research and R. L. Haney of the Naval Post-graduate School for discussions and comments and for providing observational data; R. L. Haney in particular for pointing out the importance of the anomalous heat flux in the early version of the manuscript; E. J. Aubert and D. B. Rao of the Great Lakes Environmental Research Laboratory for their understanding and support, J. M. Kelley for editing and B. J. White and C. Kish of the Great Lakes Environmental Research Laboratory for typing. All computations were carried out at the National Center for Atmospheric Research (NCAR) computing facility. NCAR is sponsored by the National Science Foundation.

This research was supported by the Office of Naval Research for the NORPAX program through a contract with the Scripps Institution of Oceanography, University of California, La Jolla, California, and later with the University of Michigan, Ann Arbor, Michigan.

References

Arthur, R. S., 1966: Estimation of mean monthly anomalies of sea surface temperature. *J. Geophy. Res.*, 70(10), 2689-2690.

Ballis, D., 1973: Monthly mean bathythermograph data from ocean weathership PAPA, NOVEMBER, VICTOR. Scripps Inst. of Oceano. Ref. ser. 73-5, 73-6, 73-7.

Dickson, R. R., 1972: Weather and circulation of December 1971 - return to persistent temperature regime. *Mon. Wea. Rev.*, 100, 239-244.

_____, 1976: Sea surface temperature anomalies and their effect on the atmospheric circulation. In: *Proc. Joint Ocean Assembly*, September 1976, Edingburgh, Ireland.

Fofonoff, N. P., 1958: Transport Computations for the North Pacific Ocean. Manuscript rept. ser. 80. Fishery Res. of Canada. 87 p.

Haney, R. L., 1971: Surface thermal boundary condition for ocean circulation models. *J. Phys. Oceanogr.* 1, 241-248.

Haney, R. L., W. S. Shiver and K. H. Hunt, 1978: A dynamical-numerical study of the formation and evolution of large scale ocean anomalies. *J. Phys. Oceanogr.* 8(6), 952-969.

Huang, J. C. K., 1978: Numerical studies for oceanic anomalies in the North Pacific Basin: I. The ocean model and the long-term mean state. *J. Phys. Oceanogr.* 8(5), 755-778.

_____, 1979: Numerical studies for oceanic anomalies in the North Pacific Basin: II. Seasonally varying motions and structures. *J. Phys. Oceanog.* 9(1), 37-56.

Jacob, W. C., 1967: Numerical semiprediction of monthly mean sea surface temperature. *J. Geophys. Res.*, 72 (6), 1681-1689.

Namias, J., 1951: The Great Pacific Anticyclone of winter 1949-50: A case study in the evolution of climatic anomalies. *J. of Meteorol.*, 8 (4), 251-261.

_____, 1965: Macroscopic association between monthly sea surface temperature and the overlying wind. *J. Geophys. Res.*, 70 (10), 2307-2318.

_____, 1972: Experiments in objectively predicting some atmospheric and oceanic variables for the winter of 1971-72. *J. Appl. Meteorol.*, 11, 1164-1174.

Roden, G. I., 1975: On North Pacific temperature, salinity, sound velocity and density fronts and their relation to the wind and energy flux fields. *J. Phys. Oceanog.* 5, 4, 557-571.

White, W. B., and R. L. Berstein, 1978: Design of an oceanographic network in the mid-latitude North Pacific. (Submit to publication.)

White, W. B., and A. E. Walker, 1974: Time and depth scale of anomalous temperature of ocean weather stations P. N. and V in the North Pacific. *J. Geophys. Res.*, 79 (30), 4517-4522.

Wyrtki, D., 1965: The annual and semi-annual variation of sea surface temperature in the North Pacific Ocean. *Limnol. and Oceangr.*, 10 (3), 307-313.

CAPTIONS OF FIGURES

Figure 1. Simulated and observed surface temperature for the coldest and warmest months in the North Pacific Ocean (from Huang, 1979).

(a) Simulated February.

(b) Simulated August.

(c) Observed January.

(d) Observed August.

Figure 2. Simulated and observed seasonal variations of temperature at 5 stations in the mid-latitude North Pacific

(a) At ocean weathership - VICTOR (Balis, 1973)

(b) At ocean weathership - PAPA (Balis, 1973)

(c) At ocean weathership - NOVEMBER (Balis, 1973).

(d) At 45° N, 145° W and at 21° N, 135° E (Wyrtki, 1965).

Figure 3. The observed monthly mean anomalous sea level pressure patterns (from Namias, 1951).

(a) November 1949

(b) December 1949

(c) January 1950

(d) February 1950

Figure 4. Simulated anomalous surface currents (at 10 m).

(a) after 5 days of simulation

(b) after 30 days of simulation

(c) after 60 days of simulation

(d) after 90 days of simulation

Figure 5. Simulated oceanic thermal anomalies of the surface layer (10 m). Dotted area indicates negative anomaly less than 0.3° C.

(a) after 30 days of simulation

(b) after 60 days of simulation

(c) after 90 days of simulation

(d) after 120 days of simulation

Figure 6. Observed SST anomalies (from Namias, 1951). Dotted area indicated negative anomalies less than 0.5° C.

(a) November 1949

(b) December 1949

(c) January 1950

(d) February 1950

Figure 7. Observed SST anomaly for November 1971 *from Namias, 1951). Dotted area indicates negative anomalies less than 0.25° C.

Figure 8. Simulated surface layer OTA's. Dotted area indicates negative anomalies less than 0.25° C.

(a) after 30 days of simulation

(b) after 60 days of simulation

(c) after 90 days of simulation

Figure 9. Observed SST anomalies (from Namias, 1972). Dotted area indicates negative anomalies less than 0.25° C.

(a) December 1971

(b) January 1972

(c) February 1972

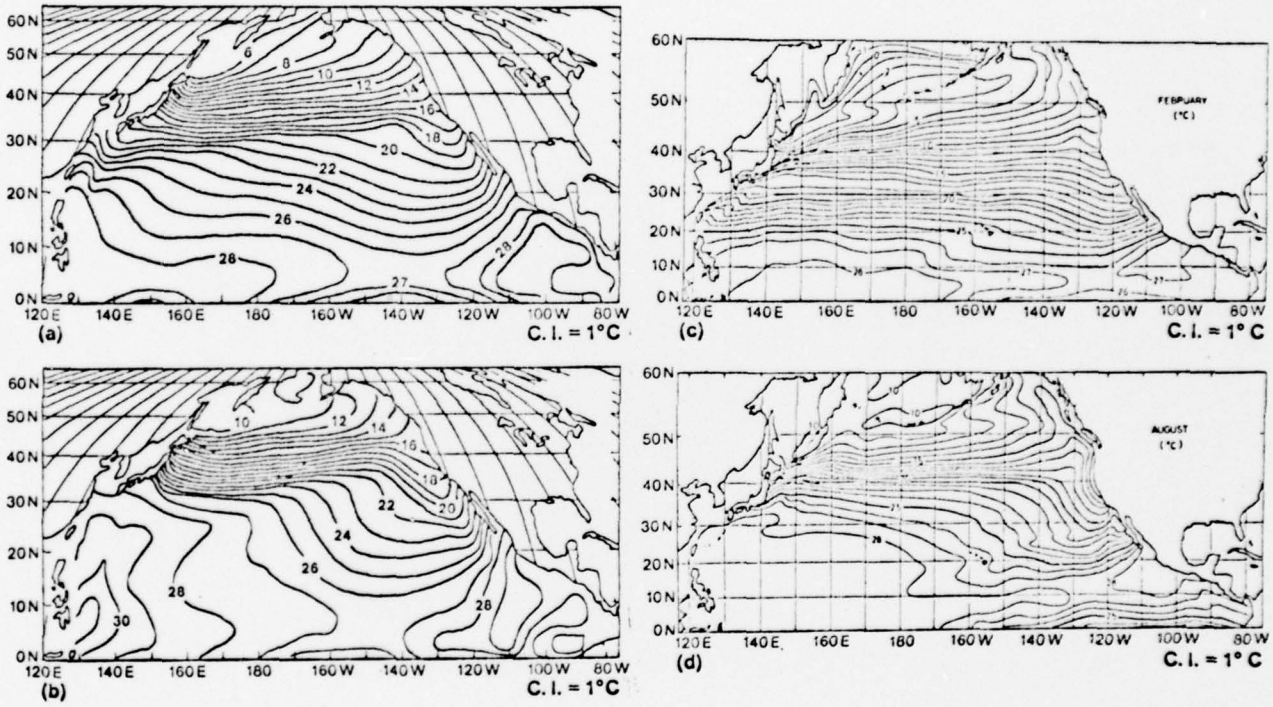
60N
50N
40N
30N
20N
10N
0N
120E
140E
160E
180
160W
140W
120W
100W
80W
(a)
C. I. = 1°C
(b)
C. I. = 1°C
(c)
FEBRUARY
(°C)
C. I. = 1° C
(d)
AUGUST
(°C)
C. I. = 1° C

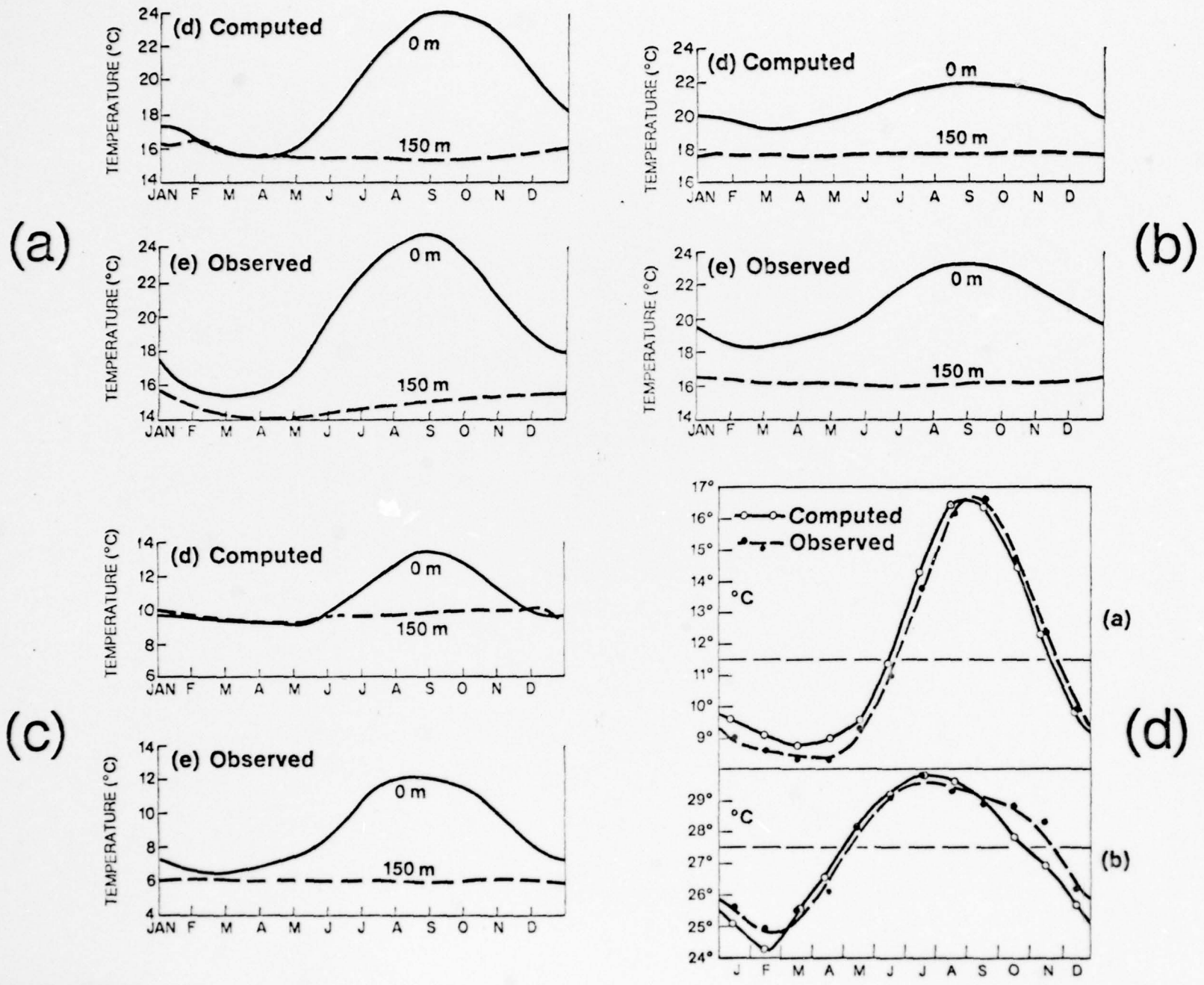
(a)
(d) Computed
0 m
150 m
TEMPERATURE (°C)
JAN F M A M J J A S O N D
(e) Observed
(b)
(c)
(d)
Computed
Observed
°C
(a)
(b)

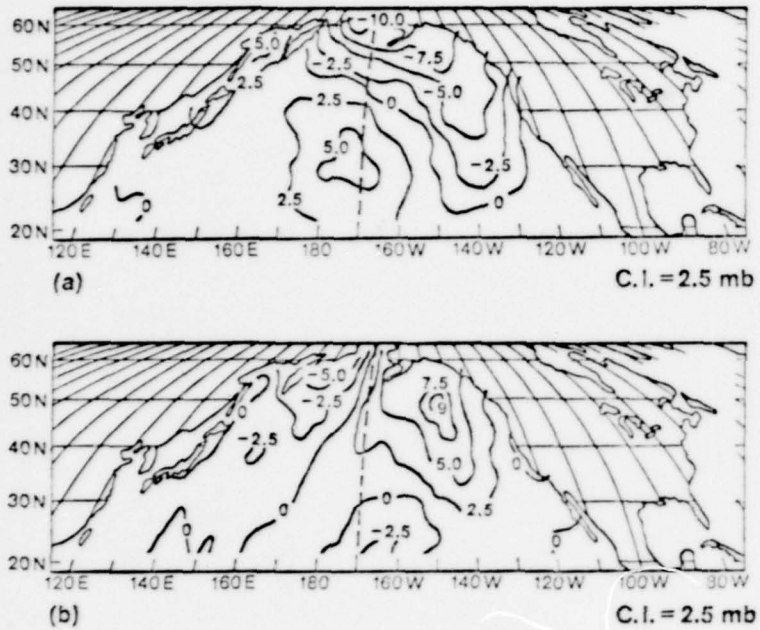

Observed SLP–

(a) November, 1949
(b) December, 1949
(c) January, 1950
(d) February, 1950

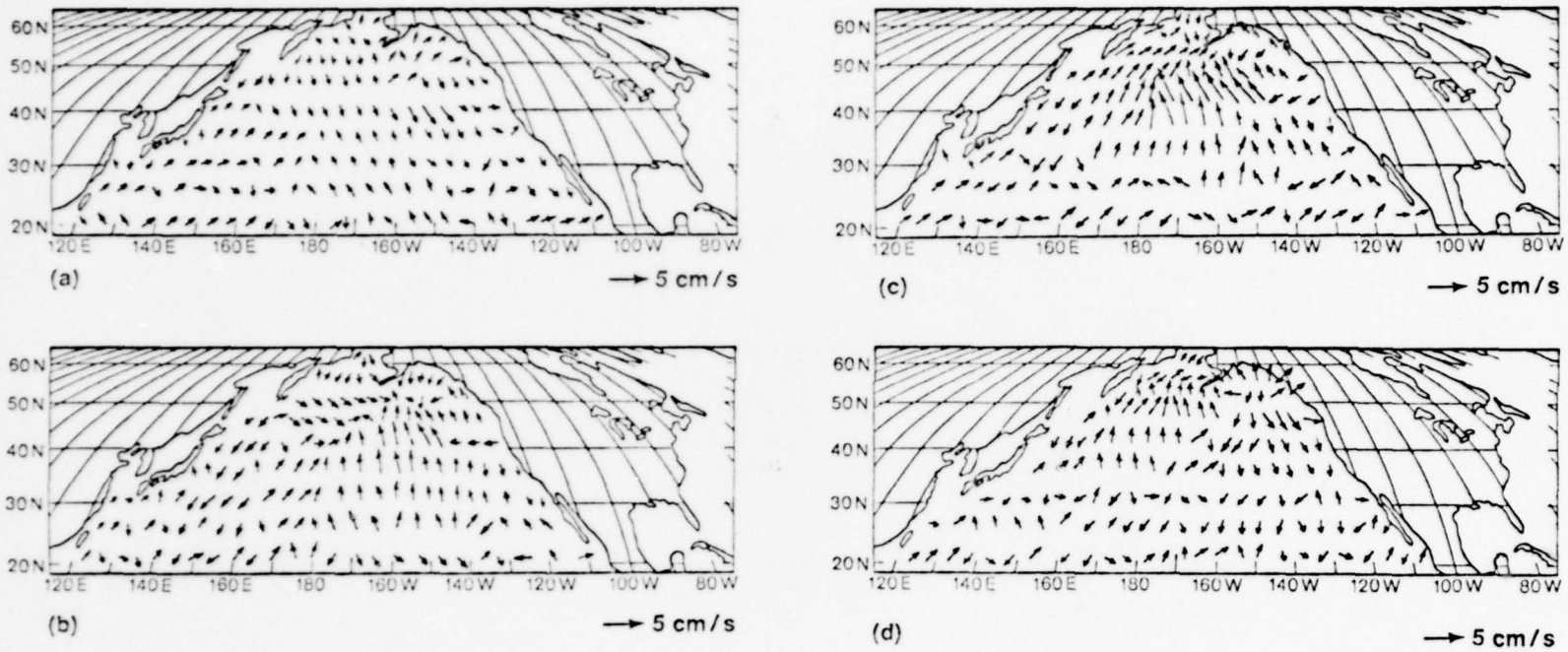

Anomalous Current Pattern (10m)

(a) after 5 days
(b) after 30 days
(c) after 60 days
(d) after 90 days

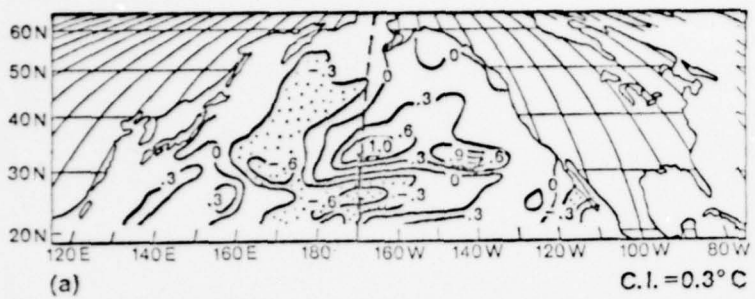

(a) C.I. = 0.3° C

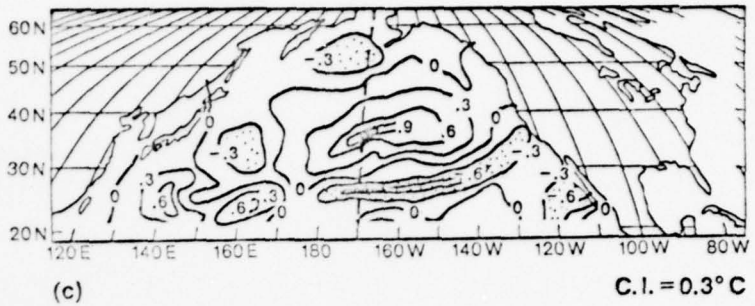

(c) C.I. = 0.3° C

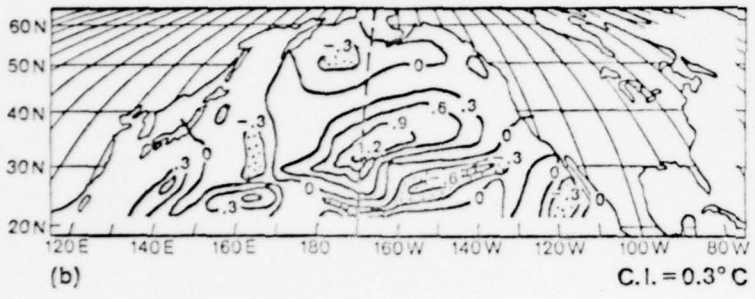

(b) C.I. = 0.3° C

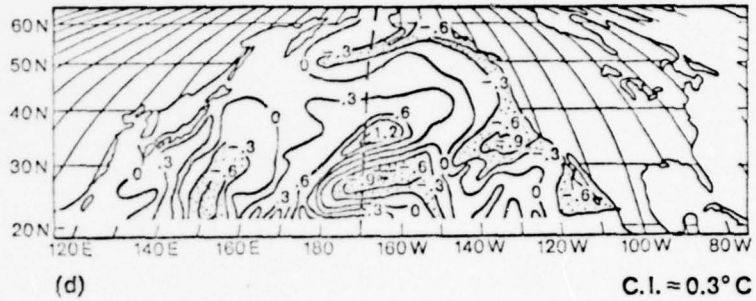

(d) C.I. = 0.3° C

Simulated OTA (10m)
(a) after 30 days
(b) after 60 days
(c) after 90 days
(d) after 120 days

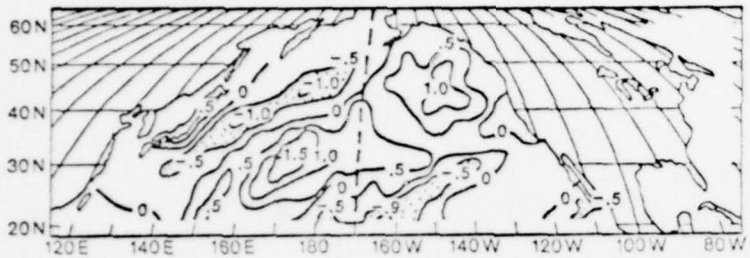

(a) C.I. = 0.5° C

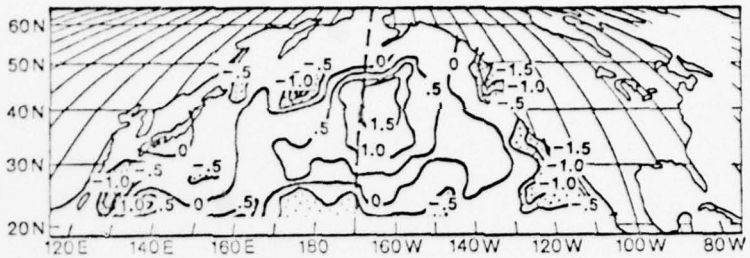

(c) C.I. = 0.5° C

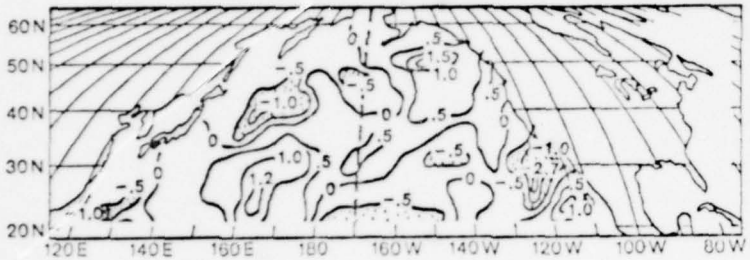

(b) C.I. = 0.5° C

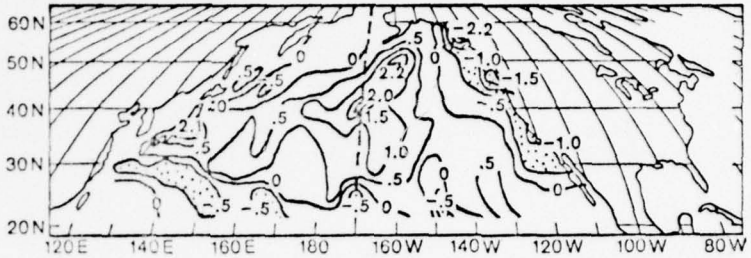

(d) C.I. = 0.5° C

Observed SST anomalies
(a) November, 1949
(b) December, 1949
(c) January, 1950
(d) February, 1950

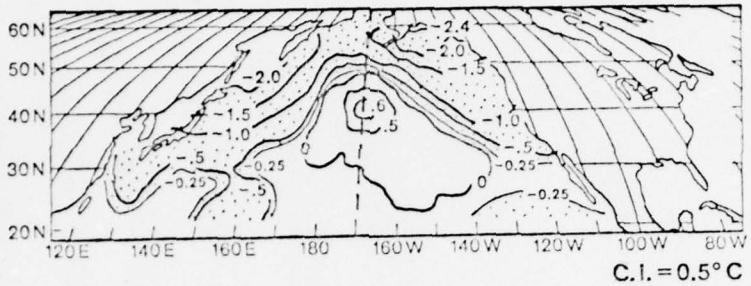

Initial Condition

The Observed Center is at (40°N, 170°W)

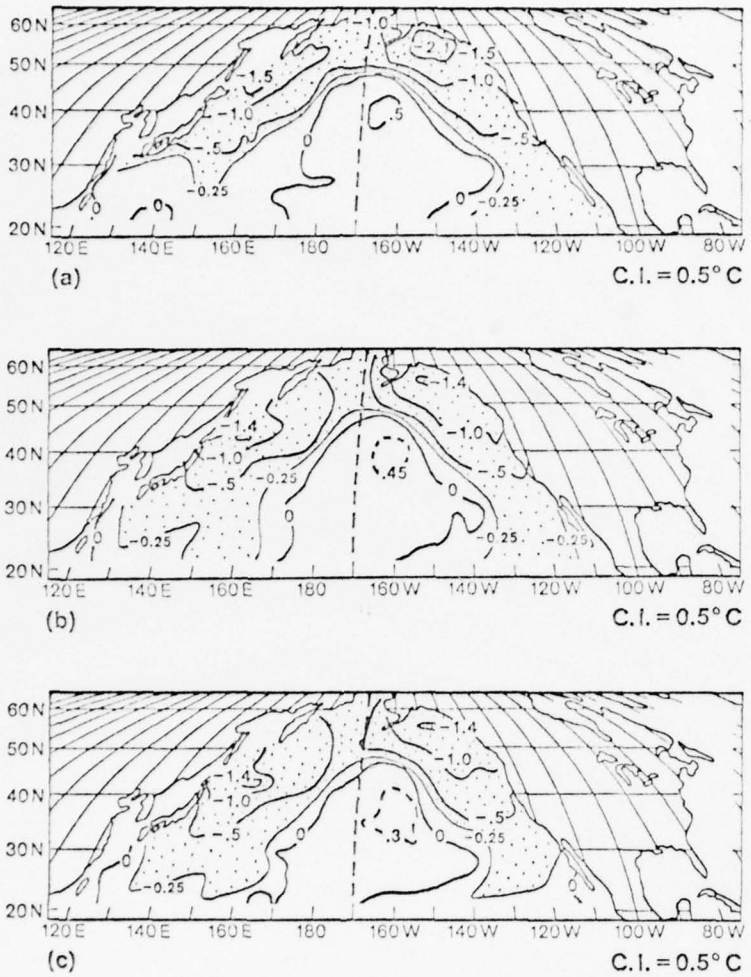

Simulated OTA's (10m)
(a) after 30 days
(b) after 60 days
(c) after 90 days

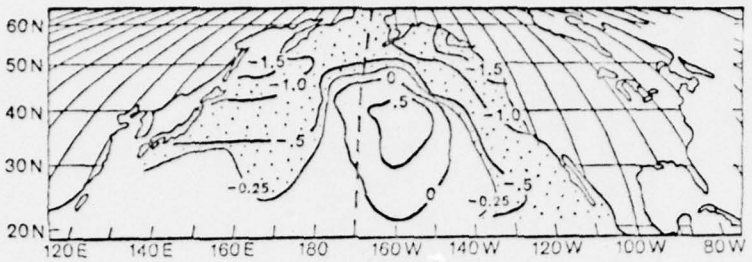

(a) C.I. = 0.5° C

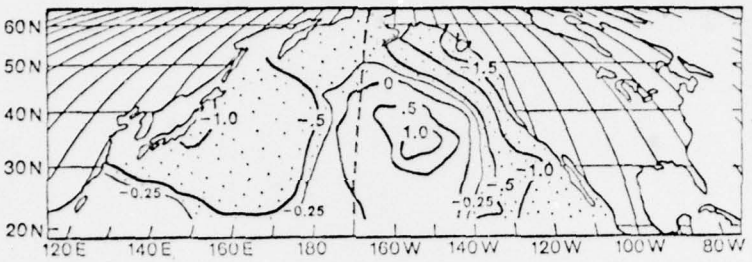

(b) C.I. = 0.5° C

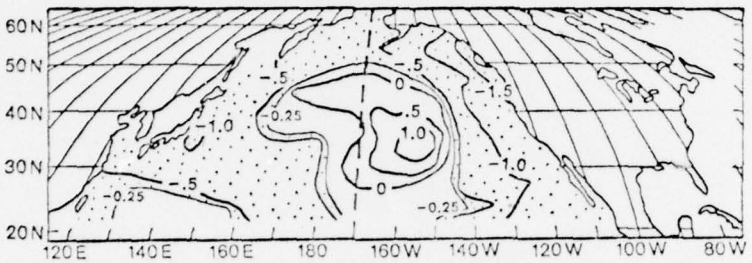

(c) C.I. = 0.5° C

Observed SST

(a) December, 1971
(b) January, 1972
(c) February, 1972